



US Army Corps  
of Engineers®

## Interactions Between Wetlands and Tidal Inlets

*by Alejandro Sánchez*

**PURPOSE:** This Coastal and Hydraulics Engineering Technical Note (CHETN) presents numerical simulations investigating how the loss of wetlands in estuaries modifies tidal processes in inlet navigation channels. The implications for wetland loss and construction of wetlands to tidal inlets and navigation channels are discussed, and hypotheses are presented for possible engineering approaches to mitigate wetland loss and improve the sedimentary sustainability of constructed wetlands.

**INTRODUCTION:** One of the navigation missions of the U.S. Army Corps of Engineers (USACE) is to maintain navigable waterways at coastal inlets and entrances. This mission requires an understanding of navigation channel shoaling; environmental relationships among the inlet, estuary, and adjacent beaches; and how modifications to the inlet and estuarine system (including placement of dredged material to create, restore, or enhance wetlands) may alter channel shoaling and adjacent morphologic features. In fiscal year 2007, the USACE dredged more than 181 million cu yd (138 million cu m) of sediment to maintain navigation through inlet, inland, and estuary channels (USACE, National Data Center 2008). The majority of this sediment is not contaminated and can be accessed to create, restore, and enhance wetlands under appropriate economic, logistical, and regulatory constraints. Placing dredged sediment to sustain environmental resources such as wetlands directly supports USACE Environmental Operating Principles to “design solutions that support and reinforce one another” and “seek to mitigate cumulative impacts to the environment” (USACE 2008).

The USACE has been involved in the creation and restoration of wetlands for more than 30 years through beneficial use of dredged material and as mitigation projects (Woodhouse et al. 1974; Garbisch et al. 1975; Landin 1982; Palermo 1992; Dunne et al. 1998; Yozzo et al. 2004). New and restored wetlands are usually designed by optimizing their functionality (benefit or performance) as determined by the hydrology hydraulics, sediment transport, water quality, and wildlife support. Wetland establishment and restoration are long-term processes that depend on sustained and conducive physical, chemical, and geological conditions. These conditions are influenced by estuary-wetland interactions such as water storage and sediment pathways. These interactions have been little explored in the design and restoration of wetlands and in the design and functioning of inlets and navigation channels. As discussed in this CHETN, the coverage, extent, and density of vegetation associated with estuarine wetlands influence the long-term evolution of estuary morphology and tidal inlets, navigation channels, and the wetlands themselves. This knowledge will be translated into predictive morphological tools for management of navigation channels and tidal inlets as part of the Estuaries and Channels Work Unit of the Coastal Inlets Research Program (CIRP).

**WETLANDS AND ESTUARINE DYNAMICS:** A leading influence of wetlands on estuaries is their contribution to determining the tidal prism (the volume of water entering an inlet during flood tide or exiting an inlet during ebb tide). As wetlands are lost or restored, the tidal prism is modified. Changes in tidal prism have several implications on the estuarine hydrodynamics and, consequently, sediment transport and morphology. Many inlets serve as navigation routes for commercial and recreational vessels. An increased tidal prism caused by wetland loss increases current velocity through the tidal inlet, thereby increasing the inlet cross-sectional area and sometimes opening new permanent or ephemeral inlets. Conversely, the development or construction of wetlands within an estuary reduces bay area and the tidal prism, which will change the phase and magnitude of the ebb and flood tides. The non-uniform change in tidal prism within the estuary can significantly alter the circulation pattern and create new channels and fill in existing ones (FitzGerald et al. 2004). Wetlands can be restored by opening (breaching) diked sections of the shore. Breached restoration sites have been linked to an increase in estuarine cross-sectional area and erosion of the existing salt marsh (Pethick 2002).

Tidal wetlands also influence estuarine dynamics by producing tidal asymmetry. For marsh platforms that lie above low tide elevation, the increased flow resistance by wetland vegetation during high tides (as compared to no resistance at low water) produces longer, but weaker flood tides and shorter, but stronger ebb tide—called ebb dominance (Boon and Byrne 1981; Speer and Aubrey 1985; Friedrichs and Aubrey 1988). By continuity of mass, the current velocity at an inlet is directly proportional to the rate at which the tidal prism changes with water elevation. The convex bathymetric profile associated with wetlands produces an increased rate of change in tidal prism during ebb tide, enhancing ebb dominance (Boon 1975; Dronkers 1986). Because sediment transport is proportional to the current velocity to a power greater than one, tidal asymmetry determines the net direction of the depth-averaged sediment transport flux. Therefore, flood-dominant systems will have a net import of sediments, whereas ebb-dominant systems will have a net export of sediments. The influence of wetlands on tidal asymmetry depends on the extent of wetland coverage, the tidal amplitude, the size of estuary, and other factors. Earlier studies of tidal asymmetry in estuaries have consisted of analytical solutions or numerical simulations of simplified geometries and semi-diurnal tides (Speer and Aubrey 1985; Friedrichs and Aubrey 1988; Lawrence et al. 2004; Fortunato and Oliveira 2005). To improve understanding of the interactions between wetlands and their inlets and channels, it is necessary to study estuaries under mixed tide and with realistic bathymetry and geometry. This CHETN is intended to be a step beyond the previous work in that it applies a two-dimensional (depth-averaged) circulation model to an idealized estuary with a bathymetry and geometry that more closely resemble the natural system.

During storms, coastal wetlands dissipate wave energy, reducing shore and bay bottom erosion, thus preserving the tidal prism and augmenting the functioning of shore-protection structures during storms (Owen 1984; Moeller et al. 1996). Wetlands and complex channel networks absorb tidal energy and reduce tidal amplitudes and currents. In addition, vegetation roots shelter and reinforce bottom sediments to protect the area from erosion (Coops et al. 1996). Wave setup contributes to elevated water level during storms and can account for a considerable part of total storm water level. Analytical work of Dean and Bender (2006) recently showed that vegetation can significantly reduce wave setup and even produce a setback.

Wetlands are a significant part of the regional sediment budget, in which they serve as sediment sinks even in ebb-dominated tidal regimes. For example, Ganju et al. (2005) estimated a net import of 14 metric tons over a 34-day period in two ebb-dominated tidal channels in a small marsh island in San Francisco Bay, CA. Wolaver et al. (1988) measured suspended sediment flux of 827 g/m<sup>2</sup>/year into a marsh in North Inlet, SC. The influence of wetland loss on the regional sediment distribution is poorly understood. A large portion of the sediment accretion in marshes is produced in situ by low-ground production (mostly from vegetation). In some estuaries, the resuspension and advection of marsh sediments are related to episodic meteorological phenomena such as tropical storms and frontal passages. Baumann et al. (1984) found that 70 to 80 percent of the accreted sediment in Barataria Bay, LA, salt marshes was deposited during winter frontal passages. Stumpf (1983) also found similar storm-dominated sediment deposition in Delaware Bay marshes. It is generally accepted that, when wetlands erode, most of the fine sediments are transported offshore and removed from the littoral system. Determining sediment loss and gain in estuaries during typical and severe storms is necessary to estimate long-term estuarine evolution.

Wetland processes and their interactions with tidal inlets and navigation channels must be integrated to predict long-term morphological evolution. This CHETN illustrates how idealized numerical modeling can be used to examine and quantify these interactions and reveal areas lacking knowledge for further model development.

**LONG-TERM EXPERIENCE:** Data spanning more than 100 years in Barataria Bay, LA, illustrate how wetland loss can modify tidal prism, inlet area, and ultimately the regional sediment budget. Because of rapid relative sea level rise (1.03 cm/year), wetland loss, and erosional processes within Barataria Bay, the bay area increased more than 775 km<sup>2</sup> from 1956 to 1990. The resulting increase in bay area increased the tidal prism through the four inlets fronting the estuary, and increased the inlet cross-sectional areas and shoal volumes. For example, the ebb-tidal shoal at Barataria Pass moved more than 2.2 km seaward from 1880 to 1980, the inlet cross-sectional area increased from 4,200 to 6,900 m<sup>2</sup>, and the pass deepened from 14 to 37 m. Sediment to build the expanding ebb tidal shoals originated from deepening of the inlets, the longshore sediment transport system, and the adjacent barrier islands. Thus, wetland loss and relative sea level rise ultimately resulted in a sink to the regional sediment budget (FitzGerald et al. 2004).

In multiple inlet-bay systems, wetland loss can switch the dominant inlet and change the regional sediment transport pattern. For example, the greater loss of wetlands in the northern part of Barataria Bay directed a larger proportion of the tidal prism through Barataria Pass with respect to Caminada Pass, Pass Abel, and Quatre Bayou Pass, and eventually realigned the channel to a more north-south alignment. The change in channel orientation caused the ebb tidal shoal to shift further east, eventually providing more protection to the western Grand Isle barrier island (FitzGerald et al. 2004). This long-term data set at Barataria Bay lends insight into the possible role wetlands can play in changing tidal prism, inlet cross-sectional area, and flow through inlet channels for the benefit of navigation and, in this case, for reducing operation and maintenance costs. Due to relative sea level rise, wetland loss is expected to increase in Barataria Bay as in many other locations. The Barataria-Terrebone Ecological Landscape Spatial Simulation model predicts an almost 90 percent wetland loss in the Barataria Basin from 1988 to 2018 for the present rate of sea level rise (Martin et al. 2002).

**NUMERICAL EXPERIMENT:** The change in current velocity at tidal inlets caused by wetland loss is examined here through numerical modeling with five idealized estuaries representing varying degrees of wetland coverage. The hydrodynamics are simulated with the Coastal Modeling System (CMS) circulation model CMS-Flow (Buttolph et al. 2006) that solves the conservative form of the non-linear shallow-water equations. The CMS is being developed under the CIRP and can interactively simulate waves, circulation, sediment transport, and morphology change.

**Idealized Estuaries.** The geomorphic classification of estuaries consists of four main groups: (1) coastal plain or drowned river valley estuaries (e.g., Chesapeake Bay, MD), (2) lagoonal or bar-built estuaries (e.g., Laguna Madre, TX), (3) fjord-type (e.g., Penobscot Bay, ME), and (4) tectonically created estuaries (e.g., San Francisco Bay, CA) (Pritchard 1967). This CHETN discusses lagoonal or bar-built estuaries (Figure 1). It is hypothesized that these estuaries are likely to be most affected by relative sea level rise and wetland loss because of their shallow water, narrow coastal inlets, and extensive wetlands.

The following parameters were considered in the design of the idealized estuaries: (1) geomorphic classification, (2) basic dimensions of width, length, surface area and depth, (3) ratio of tidal amplitude to average bay depth (relative tidal amplitude), (4) variation of the water surface area with depth (called the hypsometry), (5) ratio of volume of water over wetland to bay water volume, and (6) ratio of wetland area to bay area.

The idealized estuary shape is approximated by a semi-ellipse with two 500-m-wide sand bars and a single tidal inlet between them (Figure 2). The estuary is medium sized with a total area of 40 km<sup>2</sup>. The offshore bathymetry follows an equilibrium profile for a median sediment size of 0.1 mm. The inlet length and width are 500 and 220 m, respectively. The tidal amplitude is 0.5 m (micro-tidal) and the bay depth is 4 m (relative tidal amplitude = 0.125).

Seelig and Sorensen (1978), Boon (1975), and Boon and Byrne (1981) showed that the rate at which the wetted basin surface area varies with depth or hypsometric variation is a key factor controlling tidal flows and tidal asymmetry. The wetted surface area as a function of the water depth is given by the idealized curve (Boon 1975),

$$A' = \frac{r(1-G)}{r+G(1-r)} \quad (1)$$

in which  $A' = (A - A_{\min})/(A_{\max} - A_{\min})$ ,  $A$  is the wetted surface area at water elevation  $h$ , and  $A_{\max}$  is the wetted surface area at water depth  $h_{\max}$ . The fitted coefficient  $r = A_{\min}/A_{\max}$ , where  $A_{\min}$  is the minimum area at relative height. The parameter  $G = (1 - h')^\gamma$ , in which  $\gamma$  is a positive exponent (shape factor) that determines the shape of the curve, and  $h' = (h - h_{\min})/(h_{\max} - h_{\min})$ , where  $h_{\min}$  and  $h_{\max}$  are the minimum and maximum values of  $h$  (i.e.,  $h_{\min}$  = mean low water (MLW) and  $h_{\max}$  = mean high water (MHW)). Figure 3 shows how the Equation 1 varies as a function of  $r$  and  $\gamma$ .

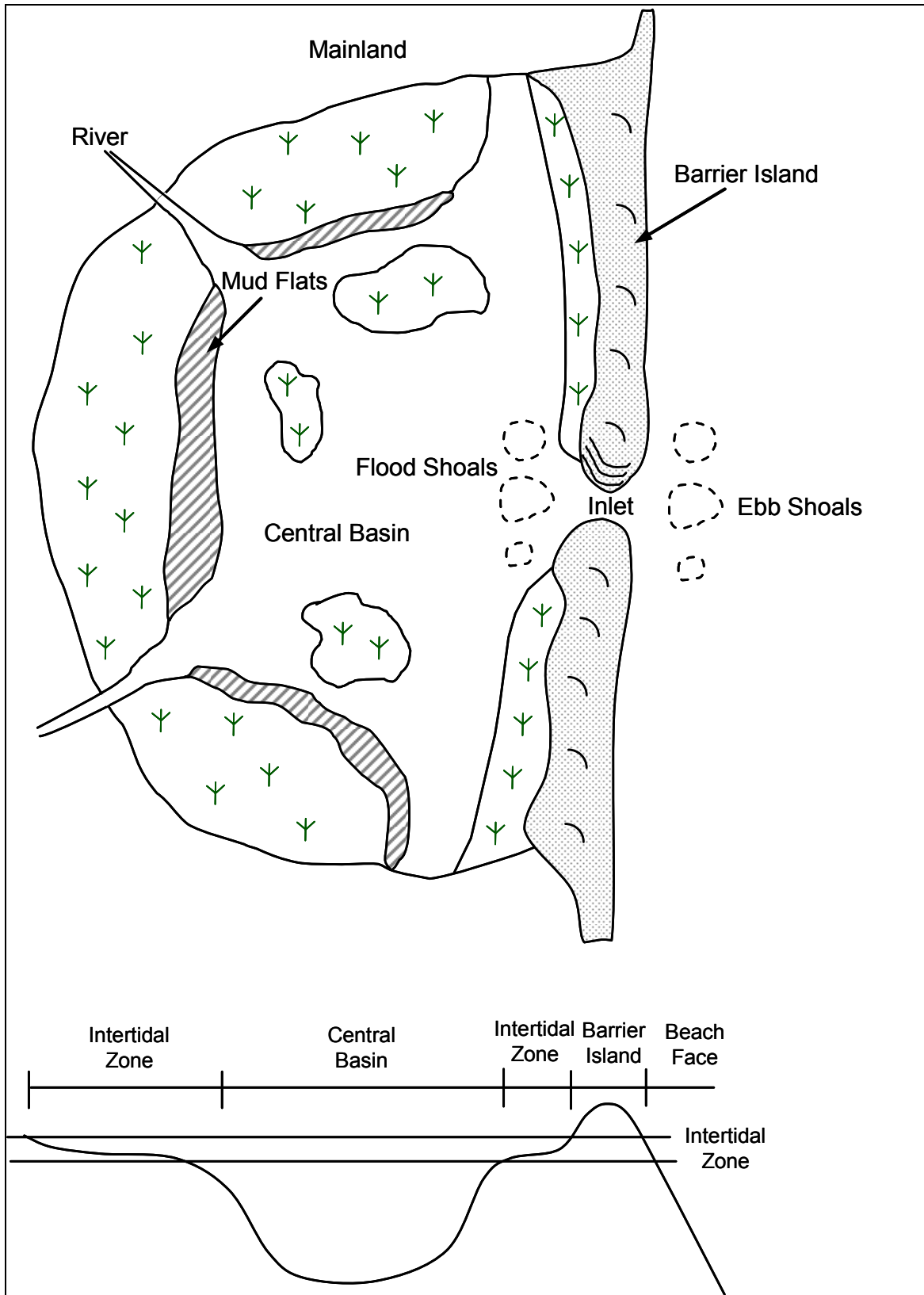


Figure 1. Plan- and cross-sectional view of a backbarrier estuary.

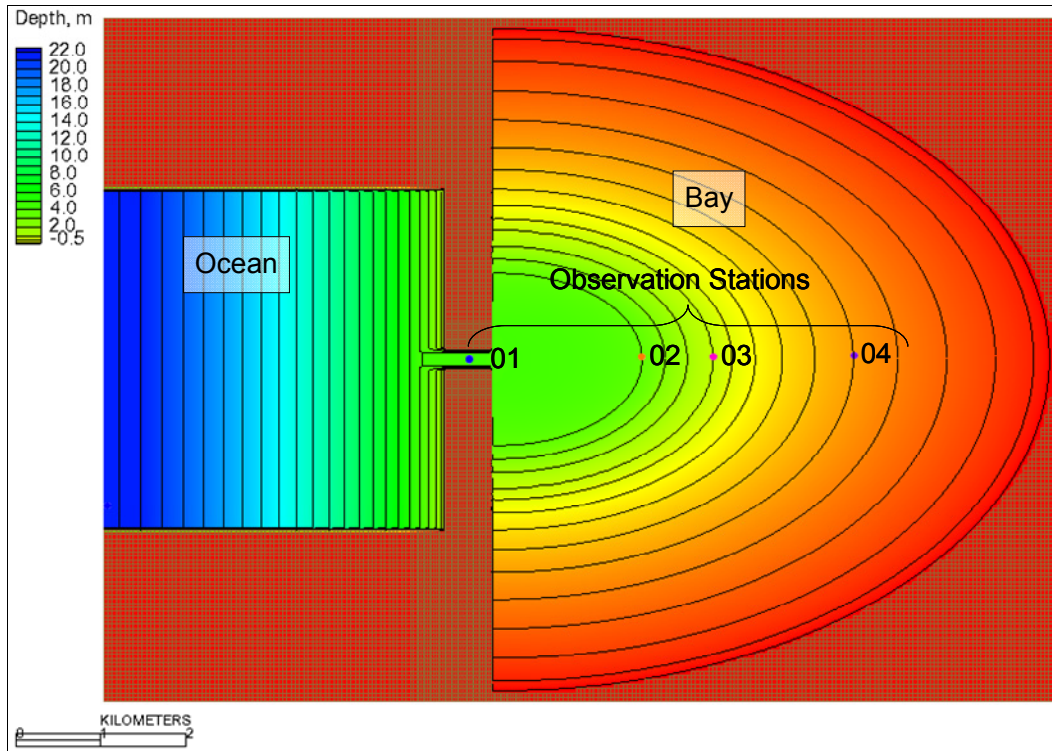


Figure 2. Idealized backbarrier estuary ( $r = 0.15$  and  $\gamma = 2$ ). Depth is relative to mean sea level, and square cells represent inactive regions.

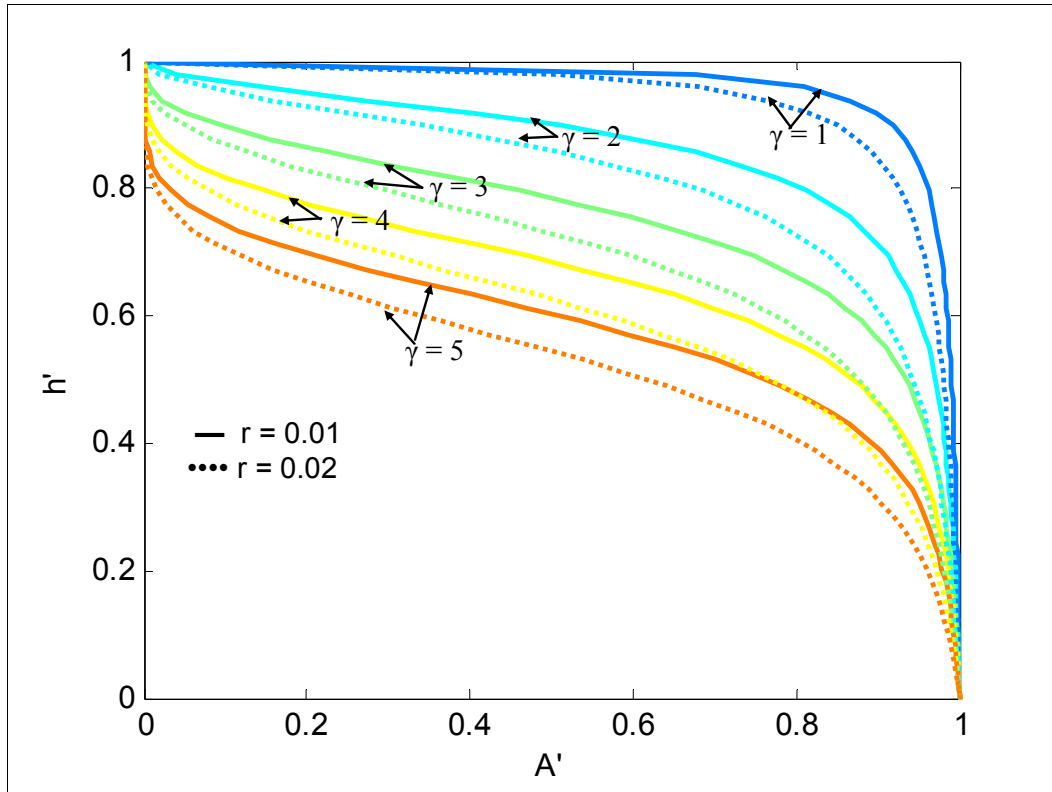


Figure 3. Idealized estuary area-height curves.

Below the intertidal range, the estuary hypsometric curve gradually approaches zero. The values for  $A_{\min}$  and  $r$  were estimated as  $11.8 \text{ km}^2$  and  $0.15$ , respectively, by comparing the percent wetland coverage and ratio of intertidal to estuarine channel water volume. These estimates are consistent with the values reported in Friedrichs and Aubrey (1988) and references therein. For  $r = 0.15$ , the shape of the hypsometric curve is approximately convex for  $\gamma < 2$  and becomes concave for  $\gamma > 2.5$ .

The change in hypsometric curve due to wetland loss is simulated by increasing the shape factor  $\gamma$ . Five numerical tests were conducted with shape factors equal to 1, 2, 4, 5, and 6. Because vegetation can grow only within a portion of the intertidal range, the amount of habitat area for vegetation decreases as the shape factor increases. As an example, Figure 3 shows the bathymetry for an idealized estuary with  $\gamma = 2$ . The fundamental assumptions here are (1) the inlet, estuary bottom, and perimeter do not change ( $r = \text{constant}$ ), and (2) for varying degrees of wetland loss, the area-depth relationship of the estuary within the intertidal zone can be approximated by Equation 1.

Stable intertidal salt marshes occupy relatively flat areas known as marsh platforms within the intertidal zone. The marsh vegetation modeled herein is intended to represent *Spartina alterniflora* or smooth cord grass, which is the most prevalent salt marsh vegetation in the United States. The range of *S. alterniflora* depends mostly on the mean range of tide ( $M_n$ ) defined as  $M_n = \text{MHHW} - \text{MLLW}$ . For the modeling discussed herein, the upper and lower elevation limits of vegetation are calculated as  $z_{\text{upper}} = 0.43M_n + 0.25$ , and  $z_{\text{lower}} = -0.24M_n + 0.09$ , respectively, from Mckee and Patrick (1988). As an example, the vegetation distribution for the idealized estuaries with  $\gamma = 2$  is shown in Figure 4. Stem densities of *S. alterniflora* vary both spatially within a marsh and from region to region and range from 16 to 4,080 stems/ $\text{m}^2$ , but are typically in the range of 50 to 350 stems/ $\text{m}^2$  (Visser et al. 1996 and references therein). Here, a relatively dense salt marsh density of 320 stems/ $\text{m}^2$  is used with an average stem diameter of 0.2 cm and is constant over the vegetated salt marsh (Leonard and Luther 1995; Lightbody and Nepf 2006).

**Vegetation Flow Drag.** The estimation of vegetation flow drag is not straightforward in a regional model because of the variation in plant density and micro-topography. First- and second-order tidal channels within the marsh have the effect of reducing flow drag. The vegetation flow drag usually requires field measurements for calibration. Vegetation flow drag should be represented in a physically reasonable form and not by simply increasing the bottom friction. Bottom friction decreases as the water depth increases, whereas the opposite is true for vegetation flow drag. Here, vegetation is modeled as rigid vertical cylinders, and a correction is applied to compensate for the presence of tidal channels. Vegetation flow drag is estimated as (Wu and Wang 2004)

$$\tau_v = \alpha_c \frac{1}{2} C_d \rho_w \lambda_a |U|U \quad (2)$$

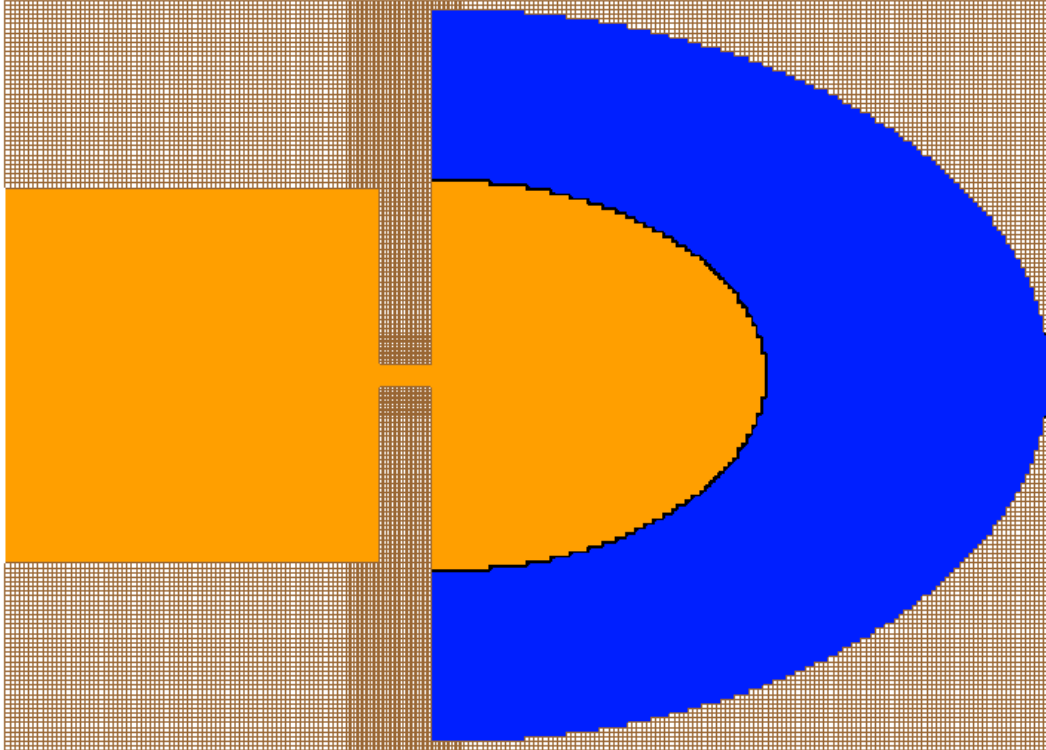


Figure 4. Example vegetation coverage for an idealized backbarrier estuary ( $r = 0.15$  and  $\gamma = 2$ ). Blue areas represent a vegetation density of 320 stems/m<sup>2</sup> and square cells represent inactive regions.

where  $\alpha_c$  is a correction factor for the presence of a tidal channel network (approximated here as the ratio of vegetated marsh platform area to total marsh area),  $C_d$  is an empirical bulk drag coefficient (set to 1.0),  $\rho_w$  is the water density,  $\lambda_a$  is the vegetation projection area per unit volume, and  $U$  is the flow velocity vector. The projected vegetation area per unit volume is calculated as  $\lambda_a = n_v D_v \min(h_v, h)$  where  $n_v$  is the number of stems per square meter,  $D_v$  is the stem diameter,  $h_v$  is the average plant height (set to 0.75 m), and  $h$  is the local water depth. Equation 2 enters the momentum equations in a similar manner as the bottom friction.

**Model Setup.** The idealized estuary was forced with the principal lunar semidiurnal constituent  $M_2$  with an amplitude of 0.5 m. For a tidal range of 1 m, the lower and upper limits of vegetation are -0.15 m and 0.68 m with respect to mean sea level. The grid resolution varied from 25 m at the tidal inlet to 50 m elsewhere. A constant Manning's  $n$  of 0.025 was specified over the calculation domain.

**Numerical Model Results.** Example current velocities at four observation stations are shown in Figure 5 for the idealized estuaries with shape factors equal to 2 and 5, which represent vegetated areas of 69 and 36 percent (48 percent wetland loss). The results show an increase in both maximum flood and ebb current velocities at the tidal inlet of 25 and 21 percent, respectively. Increased current velocities are also observed at all other stations with ranges between 30 and 46 percent. The change in sediment transport rate would be significantly greater than the current velocity.

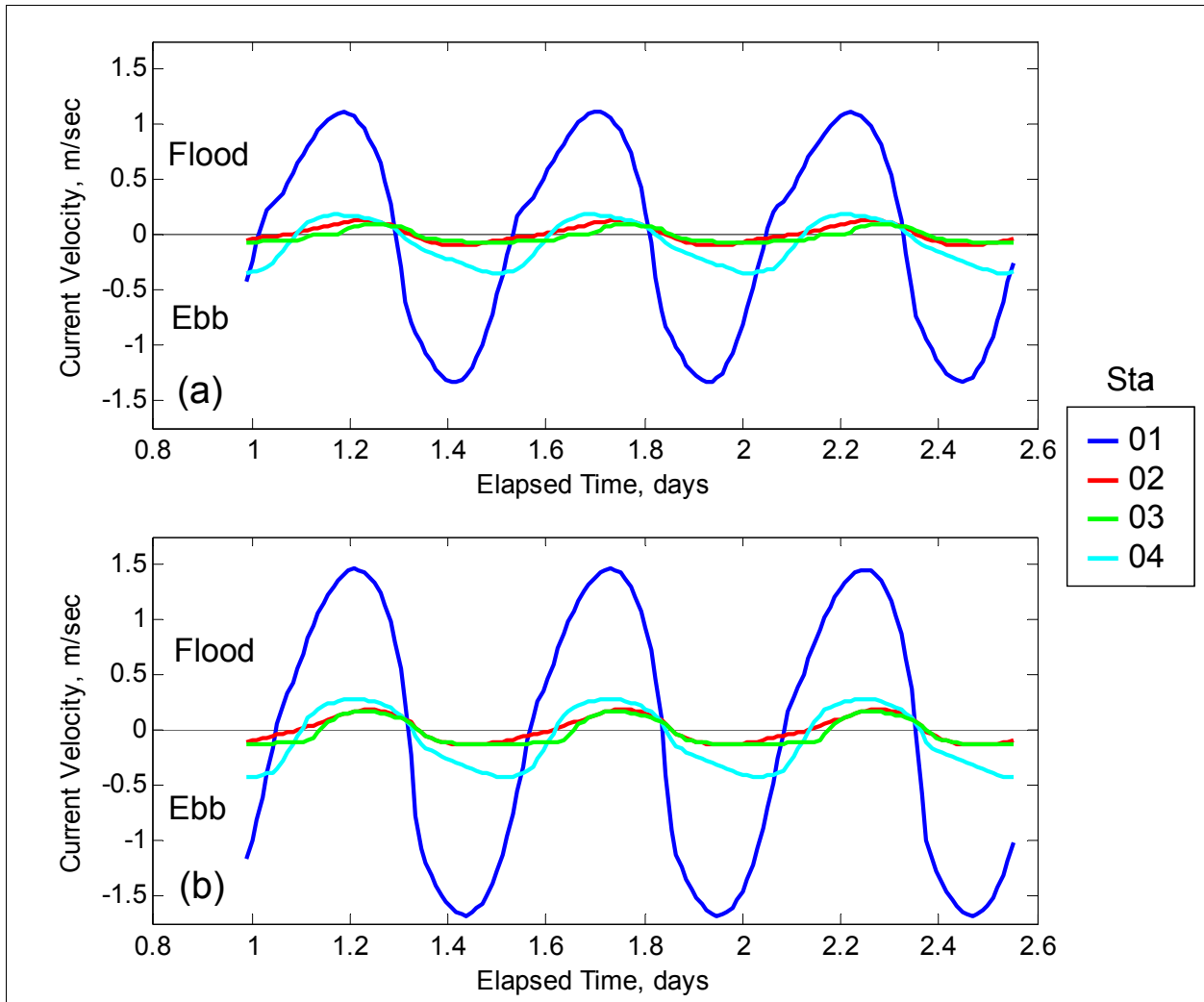


Figure 5. Current velocities in the x (flood) direction at four stations for the idealized inlet: (a) shape factor = 2, and (b) shape factor = 5.

Key numerical model parameters and a summary of results are listed in Table 1. The proportion of the bay that is covered by vegetation varies between 78 and 26 percent. The duration of the flood and ebb tides and the ratio of the maximum flood and ebb currents are relative indicators of flood and ebb dominance. The increase in tidal prism with increasing wetland loss causes an increase in both the flood and ebb current velocities through the tidal inlet. However, as the shape factor increases, the bathymetric profile becomes more concave, reducing the ebb dominance. Although all of the cases tested were ebb dominant, represented by the ratio of the maximum flood to ebb current velocity, there is a clear tendency toward flood dominance with increasing shape factor. The cases show only a slight increase (decrease) in flood (ebb) tides of 0.25 hr.

<b>Table 1</b> <b>Description of five idealized estuaries with shape factors between 1 and 6 and</b> <b>summary of current velocities at the tidal inlet (<math>n_v D_v = 0.64</math> stem/m).</b>					
<b>Parameter</b>	<b>Case A</b>	<b>Case B</b>	<b>Case C</b>	<b>Case D</b>	<b>Case E</b>
Shape factor $\gamma$	1	2	4	5	6
$100 \times A_i/A_b$ , %	78	69	47	36	26
Tidal prism, km <sup>3</sup>	48.03	60.02	72.73	76.17	78.69
$V_i/V_b$	0.79	1.17	1.48	1.52	1.52
Flood tide, hr	6.75	6.75	6.75	7.00	7.00
Ebb tide, hr	5.25	5.25	5.25	5.00	5.00
$U_{flood}$ , m/sec	0.86	1.10	1.38	1.45	1.50
$U_{ebb}$ , m/sec	1.10	1.33	1.60	1.68	1.73
$ U_{flood}/U_{ebb} $	0.79	0.82	0.86	0.86	0.87
<p><b>NOTE:</b>  <math>V_i</math> = Wetland intertidal water volume of wetland.  <math>V_b</math> = Estuarine water volume.  <math>U_{flood}</math> = Maximum flood current velocity at inlet.  <math>U_{ebb}</math> = Maximum ebb current velocity at inlet.  <math>A_i</math> = Wetland intertidal surface area.  <math>A_b</math> = Estuarine surface area.</p>					

**DISCUSSION:** Recognizing possible limits of the model assumptions, including the idealized distribution of estuarine vegetation, hypsometric curve, and simplified tidal forcing, the results of the idealized estuary simulations provide quantitative insight into how wetland loss and restoration in backbarrier bays modify current velocities at tidal inlets. Two main processes are observed. First, as the tidal prism increases due to wetland loss, there is an increase in both the flood and ebb current velocities. Second, as wetland loss occurs and the bay increases in depth, the bathymetric profile becomes more convex, decreasing ebb dominance. As the estuary becomes less ebb dominant, less sediment is exported, thereby preventing the estuary from eroding. In a similar manner, as wetlands are restored or developed naturally, the intertidal zone increases and ebb dominance is enhanced, thus increasing the export of sediment from the estuary. This interaction between estuary geometry and tidal asymmetry is a natural way by which estuaries stabilize themselves.

Actual estuaries have more complex configurations and forcing than the idealized estuaries presented here. Other factors are involved in the morphologic evolution of estuaries such as sediment inputs and relative sea level rise. For estuaries to be stable in a long-term sense they must keep up with relative sea level rise by accreting both mineral and organic material. In the case of Barataria Bay, eustatic sea level rise, erosion, and local subsidence are drowning the wetlands in place. As bay area increases, fetch increases and wind-generated waves cause marsh fringe erosion.

In this study, the vegetation density was assumed constant with respect to tidal elevation, but in nature this is not the case. Vegetation occurs most commonly at specific elevations (marsh platform). The predominant marsh elevation will vary for each location, depending on the local physical, chemical, and weather conditions. It is expected that greater vegetation densities in shallow water will enhance ebb dominance.

The idealized modeling approach described here did not include the interactions between morphology change and hydrodynamics such as shore erosion, changes in tidal inlet cross-sectional area, and evolution of ebb and flood shoals. Only the resulting change in hydrodynamics was considered for different conditions representing various degrees of wetland coverage. The inlet and bay geometry were held constant, while the change in shape of the intertidal zone for varying degrees of wetland loss was simulated using an idealized curve. It is unclear how different causes of wetland loss such as drowning and marsh fringe erosion produce different responses in the hypsometric curve. Additional simulations are needed for various bay sizes, inlet dimensions, and tidal regimes to obtain a more complete understanding of the interactions between wetlands and tidal inlets.

The following areas were identified for further study in model development:

1. Vertical distribution of wetland vegetation and how it changes tidal asymmetry.
2. Change in estuary bathymetry and geometry (area-height relationship) caused by wetland loss.
3. Interactions between long-term morphology change and hydrodynamics.
4. Influence of tidal regime and relative tidal amplitude to estuary resilience to relative sea level rise and wetland loss.
5. Influence of storms and atmospheric fronts on the overall morphological evolution of estuaries (will vary regionally).

Because flow resistance caused by vegetation is proportional to the velocity squared, wetland vegetation is most efficient at dissipating momentum in areas of stronger currents. This leads to considerations about the location of vegetation and mud flats within estuaries and wetlands. Consequently, it is hypothesized that constructing and restoring vegetated marshes in areas of relatively weak current velocities and mud flats in regions of relatively strong currents (usually occurring near tidal inlets) should promote flood dominance. These placement alternatives must be carefully evaluated to ensure that the hydraulic characteristics are adequate for the sustainability of the mud flats and wetlands, and waves and currents will not erode the project site. Tidal theory suggests that wetland channels that are more shallow and narrow while maintaining the same cross-sectional area will promote flood dominance through non-linear frictional effects. It is recommended that the functional design of constructed wetlands be supported by hydrodynamic, sediment transport, and particle-tracking models.

**CONCLUSIONS:** The long-term progression of tidal inlets and navigation channels is closely related to the evolution of estuarine wetlands through the tidal prism, sediment exchange between the open ocean and estuary, the estuary surface area as a function of bay area and depth, vegetative damping, and sediment balance. Wetland loss is expected to increase in many estuaries due to sea level rise, climate change, and reduced sediment supply. The consequences of wetland loss on the tidal inlet morphology have been observed over the past 100 years in Barataria Bay, LA. A numerical experiment of an idealized estuary demonstrates the increase in both flood and ebb current velocities and the tendency to shift toward flood dominance with increasing wetland loss. Future work will provide predictive tools and guidance on the design and maintenance of tidal inlets and navigation channels that can take into account the

interactions among wetland, tidal inlets, and navigation channels. New tools for studying estuarine-wetland interactions are under development, and user input is requested on modeling capability needs.

**ADDITIONAL INFORMATION:** This CHETN is a product of the Inlet Channels and Estuaries Work Unit of the Coastal Inlets Research Program being conducted at the U.S. Army Engineer Research and Development Center, Coastal and Hydraulics Laboratory, Vicksburg, MS. Questions about this technical note can be addressed to Alejandro Sánchez (Voice: 601-634-2027, Fax: 601-634-3433, e-mail: [Alejandro.Sanchez@usace.army.mil](mailto:Alejandro.Sanchez@usace.army.mil)). For information about the CIRP, please contact the CIRP Program Manager, Dr. Nicholas C. Kraus (Voice: 601-634-2016, e-mail: [Nicholas.C.Kraus@usace.army.mil](mailto:Nicholas.C.Kraus@usace.army.mil)). The CHETN benefited from technical reviews by Julie Dean Rosati, Dr. Kraus, and Sophie Munger. This document should be cited as follows:

Sánchez, A. 2008. *Interactions between wetlands and tidal inlets*. Coastal and Hydraulics Engineering Technical Note. ERDC/CHL CHETN-IV-72. Vicksburg, MS: U.S. Army Engineer Research and Development Center.

## REFERENCES

- Baumann, R. H., J. W. Day, and C. A. Miller. 1984. Mississippi deltaic wetland survival: sedimentation versus coastal submergence. *Science* 224:1093–1095.
- Boon, J. D. 1975. Tidal discharge asymmetry in a salt marsh drainage system. *Limnology and Oceanography* 20(1):71–80.
- Boon, J. D., and R. J. Byrne. 1981. On basin hypsometry and the morphodynamic response of coastal inlets. *Marine Geology* 40:27–48.
- Buttolph, A. M., C. W. Reed, N. C. Kraus, N. Ono, M. Larson, B. Camenen, H. Hanson, T. Wamsley, and A. K. Zundel. 2006. *Two-dimensional depth-averaged circulation model CMS-M2D: Version 3.0, Report 2: Sediment transport and morphology change*. ERDC/CHL TR-06-09. Vicksburg, MS: U.S. Army Engineer Research and Development Center.
- Coops, H., N. Geilen, H. J. Verheij, R. Boeters, and G. van der Velde. 1996. Interactions between waves, bank erosion and emergent vegetation: an experimental study in a wave tank. *Aquatic Botany* 53:187–198.
- Dean, R. G., and C. J. Bender. 2006. Static wave setup with emphasis on damping effects by vegetation and bottom friction. *Coastal Engineering* 53:149–156.
- Dronkers, J. 1986. Tidal asymmetry and estuarine morphology. *The Netherlands Journal of Sea Research* 20(2/3):117–131.
- Dunne, K. P., R. A. Mahendra, and E. Sammans. 1998. *Engineering specification guidelines for wetland plant establishment and subgrade preparation*. Technical Report WRP-RE-19. Vicksburg, MS: U.S. Army Engineer Waterways Experiment Station.
- FitzGerald, D. M., M. Kulp, S. Penland, J. Flocks, and J. Kindinger. 2004. Morphologic and stratigraphic evolution of muddy ebb-tidal deltas along a subsiding coast: Barataria Bay, Mississippi River delta. *Sedimentology* 51:1157–1178.

- Fortunato, A. B., and A. Oliveira. 2005. Influence of intertidal flats on tidal asymmetry. *Journal of Coastal Research* 21(5):1062–1067.
- Friedrichs, C. T., and D. G. Aubrey. 1988. Non-linear tidal distortion in shallow well-mixed estuaries: A synthesis. *Estuarine, Coastal and Shelf Science* 27:521–545.
- Ganju, N. K., D. H. Schoellhamer, and B. A. Bergamaschi. 2005. Suspended sediment fluxes in a tidal wetland: measurement, controlling factors, and error analysis. *Estuaries* 28(6):812–822.
- Garbisch, E. W., Jr., P. B. Woller, and R. J. McCallum. 1975. *Salt marsh establishment and development*. Technical Memorandum 52. Fort Belvoir, VA: U.S. Army Coastal Engineering Research Center.
- Landin, M. C. 1982. *Habitat development at eight Corps of Engineers sites: feasibility and assessment*. Miscellaneous Paper D-82-1. Vicksburg, MS: U.S. Army Engineer Waterways Experiment Station.
- Lawrence, D. S. L., J. R. L. Allen, and G. M. Havelock. 2004. Salt marsh morphodynamics: an investigation of tidal flows and marsh channel equilibrium. *Journal of Coastal Research* 20(1):301–316.
- Leonard, L. A., and M. E. Luther. 1995. Flow hydrodynamics in tidal marsh canopies. *Limnology and Oceanography* 40(8):1474–1484.
- Lightbody, A. F., and H. M. Nepf. 2006. Prediction of velocity profiles and longitudinal diffusion in emergent salt marsh vegetation. *Limnology and Oceanography* 51(1):218–228.
- Martin, J. F., E. Reyes, G. P. Kemp, H. Mashriqui, and J. W. Day, Jr. 2002. Landscape modeling of the Mississippi Delta. *BioScience* 52(4):357–365.
- Mckee, K. L., and W. H. Patrick, Jr. 1988. The relationship of smooth cordgrass (*Spartina alterniflora*) to tidal datums: A review. *Estuaries* 11(3):143–151.
- Moeller, E., T. Spencer, and J. R. French. 1996. Wind wave attenuation over saltmarsh surfaces: Preliminary results from Norfolk, England. *Journal of Coastal Research* 12:1009–1016.
- Owen, M. 1984. Effectiveness of saltings in coastal defense. Ministry of Agriculture, Fisheries and Food. In *Proceedings Conference of Coastal Engineers*. Cranfield, UK.
- Palermo, M. R. 1992. *Wetlands engineering: Design sequence for wetlands restoration establishment*. Wetlands Research Program Technical Note WG-RS-3.1. Vicksburg, MS: U.S. Army Engineer Waterways Experiment Station.
- Pethick, J. 2002. Estuarine and tidal wetland restoration in the United Kingdom: Policy versus practice. *Restoration Ecology* 10(3):431–437.
- Pritchard, D. W. 1967. What is an estuary: physical viewpoint. In *Estuaries, American Association for the Advancement of Science*, ed., G. H. Lauff, 3–5. Washington, DC.
- Seelig, W. H., and R. M. Sorenson. 1978. Numerical model investigation of selected tidal inlet-bay system characteristics. In *Proceedings, 14th Coastal Engineering Conference*, ASCE, 1302–1315.
- Speer, P. E., and D. G. Aubrey. 1985. A study of non-linear tidal propagation in shallow inlet/estuarine systems, Part II: Theory. *Estuarine, Coastal and Shelf Science* 21:207–224.
- Stumpf, R. P. 1983. The process of sedimentation on the surface of a saltmarsh. *Estuarine Coastal and Shelf Science* 24:599–609.

- Visser, J. M., D. E. Evers, G. O. Holm, Jr., G. O. Peterson, and C. E. Sasser. 1996. *Annual Report Environmental Monitoring Program, Louisiana Offshore Oil Port Pipeline*. New Orleans, LA: LOOP Inc.
- U.S. Army Corps of Engineers. 2008. Environmental operating principles. <http://www.hq.usace.army.mil/cepa/envprinciples.htm>.
- U.S. Army Corps of Engineers, National Data Center. 2008. Analysis of dredging costs, FY 2007. <http://www.iwr.usace.army.mil/ndc/dredge/ddcosts.htm>.
- Wolaver, T. R., R. Dame, J. D. Spurrier, and A. B. Miller. 1988. Sediment exchange between a euhaline saltmarsh in South Carolina and the adjacent tidal creek. *Journal of Coastal Research* 4:17–26.
- Woodhouse, W. W., Jr., E. D. Seneca, and S. W. Broome. 1974. *Propagation of Spartina alterniflora for substrate stabilization and salt marsh development*. Technical Memorandum 46. Fort Belvoir, VA: U.S. Army Coastal Engineering Research Center.
- Wu, W., and S. Y. Wang. 2004. A depth-averaged two dimensional numerical model of flow and sediment transport in open channels with vegetation. *Riparian Vegetation and Fluvial Geomorphology* 8:253–265.
- Yozzo, D. J., P. Wilber, and R. J. Will. 2004. Beneficial use of dredged material for habitat creation, enhancement and restoration in New York–New Jersey Harbor. *Journal of Environmental Management* 73:39–52.

*NOTE: The contents of this technical note are not to be used for advertising, publication, or promotional purposes. Citation of trade names does not constitute an official endorsement or approval of the use of such products.*